LETTER

Miniaturization of solid-state accelerator by compact low-energy-loss electron reflecting mirror

epl A Letters Journal Exploring the Frontiers of Physics

March 2015

EPL, **109** (2015) 54004 www.epljournal.org
doi: 10.1209/0295-5075/109/54004

Miniaturization of solid-state accelerator by compact low-energy-loss electron reflecting mirror

H. Lin, C. P. Liu, C. Wang and B. F. Shen

State Key Laboratory of High Field Laser Physics, Shanghai Institute of Optics and Fine Mechanics P. O. Box 800-211, Shanghai 201800, China

received 11 November 2014; accepted in final form 24 February 2015
published online 19 March 2015

PACS 41.20.-q – Applied classical electromagnetism
PACS 52.20.Dq – Particle orbits

Abstract – Effective confining particles in a finite space region where an accelerating electric field exists are very crucial to maintain an accelerator to be small sized. The mere use of a magnetic field to drive particles back into the accelerating electric field was widely applied in cyclotron but did not well control the size of the whole accelerator. A more effective mechanism of confining particles in the accelerating electric field is studied in detail here.

The importance of a high accelerating electric field to particle acceleration is self-evident. A higher accelerating electric field favors an accelerator to be small sized [1–3]. This promotes investigations on the non–solid-state acceleration mechanisms which depend on the strong electric field beyond what a conventional solid-state accelerator can sustain [4–29]. On the other hand, the difficulty in generating a sufficiently high electric field is also marked. This naturally drives one to consider repeated usage of the accelerating electric field by driving back particles into the accelerating electric field. The well-known cyclotron is a typical example embodying this idea [30].

In a cyclotron, particles out of the accelerating region are driven back by a static magnetic field. Maybe in order to maintain the particle's energy during the process of driving it back into the accelerating region, one only uses a static magnetic field to "bend" the particle back. As a result, the "bending" region is usually very space-consuming and is almost the main factor hindering the conventional solid-state accelerator from being small sized. Namely, maybe the "bending" region is far larger than the accelerating region. Using a higher magnetic field can, of course, cut down the "bending" region. This is similar to using a higher electric field to cut down the accelerating region. Also, a similar difficulty remains.

We change the idea above to achieve a small-sized conventional solid-state accelerator. That is, we do not stick to the belief that "during the process of driving it [a particle] back into the accelerating region, there should not be any energy loss". Instead, we allow little energy loss which is below the energy gain in a round of travelling through the accelerating region (denoted as E_{gain}). Thus, the energy in a longer time-scale can keep rising but the size of the "bending" region may be effectively controlled. Guided by this idea, we use both static electric field and static magnetic field to "bend" particles back into the accelerating region. We call such a "bending" region as reflecting "mirror".

An electron in this "bending" region can be described by dimensionless 3D relativistic Newton equations (RNEs)

$$d_s\left[\Gamma d_s Z\right] = 0, \tag{1}$$

$$d_s\left[\Gamma d_s Y\right] = W_B d_s X, \tag{2}$$

$$d_s\left[\Gamma d_s X\right] = -W_B\left[\eta + d_s Y\right], \tag{3}$$

where the dimensionless relativistic factor reads

$$\frac{1}{\Gamma} = \sqrt{1-\left(d_s X\right)^2-\left(d_s Y\right)^2-\left(d_s Z\right)^2}. \tag{4}$$

Moreover, E_s and B_s are the constant-valued electric and magnetic fields satisfying $E_s = \eta c B_s$; $\lambda = c/\omega$ and ω are the reference wavelength and frequency. $s = \omega t$, $Z = \frac{z}{\lambda}$, $Y = \frac{y}{\lambda}$, $X = \frac{x}{\lambda}$ are dimensionless time-space coordinates; the dimensionless intermediate parameter $W_B = \frac{\omega_B}{\omega}$ measures the strength of the magnetic field, $\omega_B = \frac{eB_s}{m_e}$ is the cyclotron frequency.

Equations (1)–(3) will lead to

$$d_s Z = 0, \tag{5}$$

$$\Gamma d_s Y - W_B X = \text{const} = C_y; \tag{6}$$

$$\Gamma d_s X + W_B\left[\eta s + Y\right] = \text{const} = C_x, \tag{7}$$

where the values of these constants (const) are determined from the initial conditions $(X, Y, Z, d_sX, d_sY, d_sZ)|_{s=0} = \left(0, 0, 0, \frac{C_x}{\sqrt{1+C_x^2+C_y^2}}, \frac{C_y}{\sqrt{1+C_x^2+C_y^2}}, 0\right)$.

Equations (5)–(7) can yield an equation set of d_sX and d_sY

$$(d_sY)^2 = [C_y + W_B X]^2 * \left[1 - (d_sX)^2 - (d_sY)^2\right], \quad (8)$$

$$(d_sX)^2 = [C_x - W_B * (\eta s + Y)]^2 * \left[1 - (d_sX)^2 - (d_sY)^2\right] \quad (9)$$

whose solution reads

$$(d_sX)^2 = \frac{[C_x - W_B * (\eta s + Y)]^2}{\left[1 + [C_y + W_B X]^2 + [C_x - W_B * (\eta s + Y)]^2\right]}, \quad (10)$$

$$(d_sY)^2 = \frac{[C_y + W_B X]^2}{\left[1 + [C_y + W_B X]^2 + [C_x - W_B * (\eta s + Y)]^2\right]}. \quad (11)$$

It is easy to verify that the solutions (10), (11) will lead to $\Gamma = \sqrt{1 + [C_y + W_B X]^2 + [C_x - W_B * (\eta s + Y)]^2}$ and, with the help of eqs. (6), (7), $d_s\Gamma = -W_B\eta * d_sX$ (*i.e.* $m_e c^2 d_t\Gamma = eEd_tX$). If the note that Γ can be formally expressed as $\Gamma = \sqrt{1 + C_y^2 + C_x^2} - W_B\eta * X$, which agrees with Takeuchi's theory [29,31], we can find the electronic trajectory being expressed as

$$\Gamma^2 = 1 + [C_y + W_B X]^2 + [C_x - W_B * (\eta s + Y)]^2, \quad (12)$$

or

$$\left(1-\eta^2\right)\left[X + \frac{(\eta + \upsilon_{y0})}{1-\eta^2}\frac{\Gamma_0}{W_B}\right]^2 + \left[(Y + \eta s) - \upsilon_{x0}\frac{\Gamma_0}{W_B}\right]^2 = \frac{\left[(\eta + \upsilon_{y0})^2 + \left(1-\eta^2\right)\upsilon_{x0}^2\right]}{1-\eta^2}\left(\frac{\Gamma_0}{W_B}\right)^2, \quad (13)$$

where $\Gamma_0 = \sqrt{1 + C_y^2 + C_x^2}$ is the initial dimensionless relativistic factor, $\upsilon_{x0} = \frac{C_x}{\Gamma_0}$ and $\upsilon_{y0} = \frac{C_y}{\Gamma_0}$ are initial dimensionless velocity components.

In the $(Y + \eta s)$-X plane, there will be an elliptical trajectory for $\eta < 1$ and a hyperbolic one for $\eta > 1$ [29]. The time history can be exactly calculated by re-writing eq. (10) as

$$\pm \mathrm{d}s = \frac{\frac{1}{W_B}\Gamma_0 - \eta * X}{\sqrt{aX^2 + bX + c}}\mathrm{d}X = \frac{\eta}{\sqrt{a}}\frac{X_N - X}{\sqrt{\left(X + \frac{b}{2a}\right)^2 - \frac{b^2-4ac}{4a^2}}}\mathrm{d}X, \quad (14)$$

where $a = \left(\eta^2 - 1\right)$, $b = -2\left[\eta\sqrt{1 + C_y^2 + C_x^2} + C_y\right]\frac{1}{W_B}$, $c = C_x^2\left(\frac{1}{W_B}\right)^2$ and $X_N = \frac{1}{\eta}\frac{1}{W_B}\Gamma_0$ are intermediate variables introduced for simplicity purpose. Equation (14) is in a more general form

$$\pm \mathrm{d}s = \sigma\frac{M - u}{\sqrt{u^2 - 1}}\mathrm{d}u, \quad (15)$$

where $u = \frac{X + \frac{b}{2a}}{\sqrt{\frac{b^2-4ac}{4a^2}}} = \frac{X - \frac{X_R + X_L}{2}}{X_R - X_L}$, $X_L = \min(\frac{-b-\sqrt{b^2-4ac}}{2a}, \frac{-b+\sqrt{b^2-4ac}}{2a})$ and $X_R = \max(\frac{-b-\sqrt{b^2-4ac}}{2a}, \frac{-b+\sqrt{b^2-4ac}}{2a})$ are left and right ends of the regime $(\frac{-b-\sqrt{b^2-4ac}}{2a}, \frac{-b+\sqrt{b^2-4ac}}{2a})$ in the X-axis. In addition, $\sigma = \frac{\eta}{\sqrt{a}}\sqrt{\frac{b^2-4ac}{4a^2}}$ and $M = \frac{X_N + \frac{b}{2a}}{\sqrt{\frac{b^2-4ac}{4a^2}}} = \frac{X_N - \frac{X_R + X_L}{2}}{X_R - X_L}$ are also intermediate variables for simplicity purpose. Clearly, for the $a > 0$ case, it should be $u < -1$ or $u > 1$. It is easy to verify that for $\eta^2 - 1 > 0$, $M = -\frac{1 + \eta\upsilon_{y0}}{\eta\sqrt{(\eta + \upsilon_{y0})^2 + (1-\eta^2)\upsilon_{x0}^2}} < 0$. Initially, $(X, Y)\,|_{s=0} = (0, 0)$ and hence $u_{st} = \frac{0 + \frac{b}{2a}}{\sqrt{\frac{b^2-4ac}{4a^2}}} = \frac{-(\eta + \upsilon_{y0})}{\sqrt{(\eta + \upsilon_{y0})^2 + (1-\eta^2)\upsilon_{x0}^2}}$. A strict and reasonable solution reads: For u rising from u_{st} to -1, it is $\mathrm{d}s = -\sigma\frac{M-u}{\sqrt{u^2-1}}\mathrm{d}u$ and hence $s(u) = s_1(u) = \sigma * \left\{M * \log(\sqrt{u^2 - 1} - u) + \sqrt{u^2 - 1}\right\} - s_{st}$, where $s_{st} = \sigma * \left\{M * \log(\sqrt{u^2 - 1} - u) + \sqrt{u^2 - 1}\right\}|_{u=u_{st}}$ and $s_1(u = -1) = -s_{st}$. For u decreasing from -1 to $-\infty$, it is $\mathrm{d}s = \sigma\frac{M-u}{\sqrt{u^2-1}}\mathrm{d}u$ and hence $s(u) - s_1(u = -1) = s_2(u) = \sigma * \left\{-M * \log(\sqrt{u^2 - 1} - u) - \sqrt{u^2 - 1}\right\}$. Here, the choice of the sign at the left-hand side of eq. (15) is described as follows: When u rises from u_{st} to -1, the chosen sign should ensure the solution of eq. (15) to correspond to an ascent of s. Therefore, for u rising from u_{st} to -1, a "$-$" is reasonable in eq. (15) (because for the parameter values υ_{x0} and υ_{y0} we considered, "+" will correspond to $s(u) = \sigma * \left\{-M * \log(\sqrt{u^2 - 1} - u) - \sqrt{u^2 - 1}\right\}$ – const which decreases with respect to u rising from u_{st} to -1). Namely, even though it is always $M - u_{st} = \frac{\eta - \frac{1}{\eta}}{\sqrt{(\eta + \upsilon_{y0})^2 + (1-\eta^2)\upsilon_{x0}^2}} > 0$, $\mathrm{d}s = \sigma\frac{M-u}{\sqrt{u^2-1}}\mathrm{d}u$ cannot *always* warrant a solution of s rising with respect to u (from u_{st} to -1).

Y can be expressed in terms of u (from $u = u_{st}$ to $u = -1$): $Y = \sqrt{c} - \sqrt{aX^2 + bX + c} - \eta s = \sqrt{c} - \frac{a}{\eta}\sigma * \sqrt{u^2 - 1} - \eta s(u)$ and hence corresponds to a curve in the u-Y plane or the X-Y plane. Note that both X and Y can be normalized to $\frac{\Gamma_0}{W_B}$. Moreover, from $u = -1$ to $u = -\infty$, there is a different formula $Y = \sqrt{c} + \sqrt{aX^2 + bX + c} - \eta s$.

According to eq. (13), the trajectory in the $(Y + \eta s)$-X plane is a hyperbola. The trajectory in the X-Y plane will be the envelope of those hyperbolas at different values of s. Note that in the X-Y plane, the hyperbola described by eq. (13) has a time-dependent center position (the Y-coordinate of the center is $\upsilon_{x0}\frac{\Gamma_0}{W_B} - \eta s$). Thus, a particle moving along such a hyperbola might always move in the $Y < 0$ region if the center of the hyperbola moves sufficiently fast toward the $Y = -\infty$ direction. Namely, if the center is fixed, the particle which is moving along the hyperbola will enter into the $Y > 0$ region when moving from

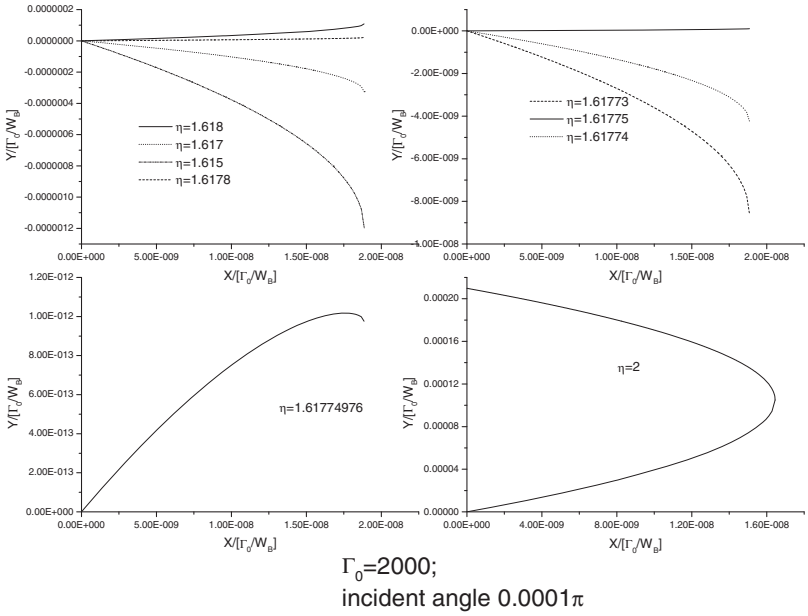

Fig. 1: Typical examples of trajectory in the X-Y plane. The trajectory starts from $(X, Y) = (0, 0)$ and is an evelope of many hyperbolas whose Y-coordinates of the centers are time dependent.

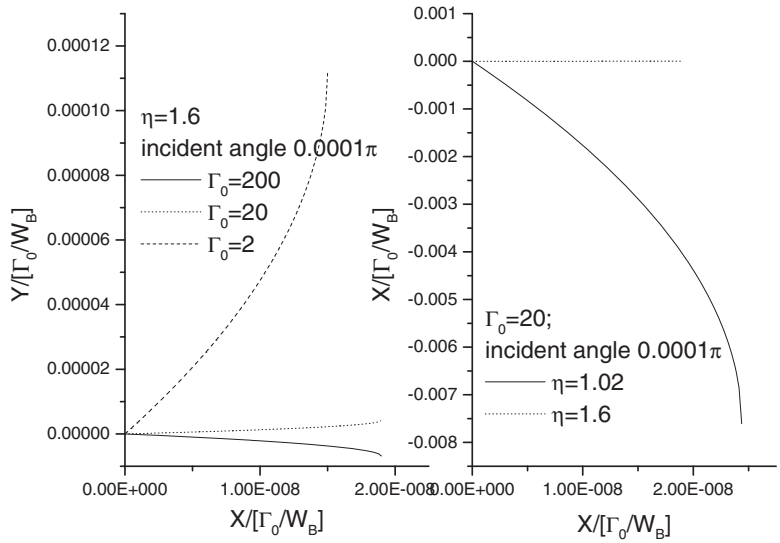

Fig. 2: The effect of parameters on the type a trajectory belongs to.

$X = 0$ to $X = X_L$. Once the center moves sufficiently fast, it is possible for the increment in the Y-coordinate due to the increment in the X-coordinate along the hyperbola with fixed center to be less than the shift in the Y-coordinate of the center. In such a situation, the particle cannot enter into the $Y > 0$ region.

As shown in fig. 1, there are 3 types of trajectory. The most common type, as shown in the bottom-right panel, shows that both X and Y rise during u evolving from u_{st} to -1, after arriving at $u = -1$, Y continues to rise (in a different formula $Y = \sqrt{c} + \sqrt{aX^2 + bX + c} - \eta s$) and X decreases. Another, or the second, common type, as represented by the downward curves in the upper two panels of fig. 1, shows that both X and Y decrease during u evolving from u_{st} to -1. Between these two common types, a relatively rare type is represented by the curve in the bottom-left panel, which displays both X and Y rising during u evolving from u_{st} to $-1-\delta$ (δ is a small positive value) but Y begins to decrease from $u = -1-\delta$ to $u = -1$. Which type a trajectory belongs to depends on η, Γ_0 and the incident angle $\theta = \arctan\frac{v_{x0}}{v_{y0}}$. Figure 1 displays the effect of η on the classification of a trajectory. Figure 2 reflects the effect of Γ_0.

The practical value of the second common type is that it means a large-angle deflection, up to π, in particle motion and such a large-angle deflection can be achieved in a very small space region. According to figs. 1 and 2, those type-II trajectories have width $< 10^{-6}\frac{\Gamma_0}{W_B}$ (in both the

X-direction and Y-direction) and hence this corresponds to a very weak energy loss $\sim 10^{-6}\eta\frac{\Gamma_0}{W_B}$. In contrast, when only the magnetic field is applied, the width of an elliptical trajectory in the $\eta = 0$ case is equal to $1\frac{\Gamma_0}{W_B}$ and hence a π-deflection demands at least a $1\frac{\Gamma_0}{W_B}$-long length in one direction.

This implies that a more compact bending region and a smaller energy loss can be achieved by choosing a small incident angle and a small η-value. Small incident angle means that the static electric field applied in the "bending" region is nearly vertical to the initial direction of the electron moving in the "bending" region. Moreover, the electron should be arranged to be initially decelerated by this electric field.

To utilize this π-deflection, an electron is introduced into the "bending" region, whose Y-direction width is denoted as W_y, in a "diving" manner. The electron "dives" into the bending region with a small velocity component along the direction of B. The Y-direction position when it arrives at the surface of the E-field is denoted as L_y. By choosing $0 < L_y < W_y$, we can control the moving direction of an electron when it leaves the "bending" region. Both the acute-angled deflection and the obtuse-angled one can be achieved by controlling W_y, L_y, η, etc.

In a π-deflection, if the shift in the X-direction is too small, the deflected electron, as shown in fig. 3, will encounter a decelerator unit. Therefore, we wish the route of the deflected electron might have a not-too-small shift from that of the incident electron. If this cannot be fulfilled through a 1-step π-deflection, a 2-step π-deflection (see fig. 3) should be attempted.

Actually, a hyperbolic trajectory (in the $(Y + \eta s)$-X plane) implies a deflection angle $\pi - 2\arctan\left[\sqrt{\eta^2 - 1}\right]$. Therefore, even not pursuing the 1-step π-deflection and the 2-step one, we can still achieve a π-deflection through multiple steps (each step contributes a deflection angle $\pi - 2\arctan\left[\sqrt{\eta^2 - 1}\right]$). This requires to use some "bending" units rather than a large "bending" region. Namely, the usage of the static magnetic field B should be finer. A crude usage of B is to apply it directly on a large region. Clearly, such a crude usage is neither economic nor efficient (because a large space is required to finish a deflection at the desired angle and B is required to exist always in such a large space.) In contrast, in a finer usage mode, B and E exist in many specified space regions (*i.e.* "bending" units), but particles can freely fly outside those "bending" units. Even if there are multiple steps, the total volume required by these steps is still considerably smaller than that by merely a pure magnetic-field–induced π-deflection. The total volume required for a multi-step π-deflection will be slightly above $\frac{\pi}{\pi - 2\arctan\left[\sqrt{\eta^2-1}\right]} * \left[10^{-6*2}\right] * \left[\frac{\Gamma_0}{W_B}\right]^2$ while that for a pure magnetic-field–induced π-deflection is at least $1\left[\frac{\Gamma_0}{W_B}\right]^2$. A very significant difference in magnitude is obvious!

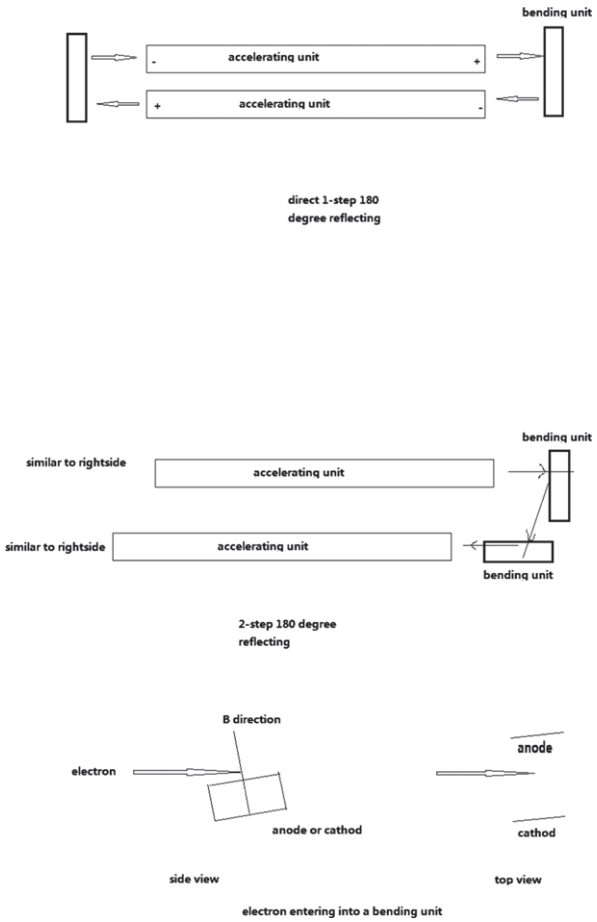

Fig. 3: Design of a compact accelerator. Two neighboring accelerating units are of opposite electric fields. The inicident angle when an electron enters a bending unit can be adjusted by rotating the bending unit. Clearly, if each bending unit contributes a small energy loss $|E_{loss}(i)| < E_{gain}$, the whole apparatus can generate higher output energy by using more stacks of such a combination of 1 accelerating unit + 2 bending units. According to the current technique level, $E_{gain} = 1\,\mathrm{MeV}$ and 1 meter long accelerating units are available.

If we do not use the above-described "diving" manner to introduce an electron into the "bending unit and instead we introduce the electron completely into the X-Y plane, we can also achieve an acute-angled deflection. According to the type-II trajectory shown in figs. 1 and 2, each type-II trajectory has a limit value of the slope, $\lim_{X\to 0}\frac{\mathrm{d}Y}{\mathrm{d}X}$. Because $E_s = 0$ and $B_s = 0$ at $Y < 0$ half-space, an electron will move, in the $Y < 0$ half-space, along this angle $\arctan\left(\lim_{X\to 0}\frac{\mathrm{d}Y}{\mathrm{d}X}\right)$. This implies a deflection angle $\arctan\left(\frac{v_{x0}}{v_{y0}}\right) + \frac{\pi}{2} - \arctan\left(\lim_{X\to 0}\frac{\mathrm{d}Y}{\mathrm{d}X}\right)$, which is an acute angle because $\arctan\left(\frac{v_{x0}}{v_{y0}}\right)$ is very small.

The values of E and B are common enough and hence easy to be achieved according to current technique condition. For example, B is about 0.1–1 T and E is about $3 * 10^{5-7}\,\mathrm{V/m}$. It is not difficult to achieve $E = 3 * 10^{2-4}\,\mathrm{V/mm}$ by adjusting the inter-plate distance and voltage. $B = 0.1\,\mathrm{T}$ corresponds to $\omega_B = 1.85 * 10^{10}\,\mathrm{Hz}$

and $\frac{\omega_B}{\omega} = \frac{1.85}{6\pi} * 10^{-4}$–$10^{-5}$ if $\omega = 3 * 2\pi * 10^{14}\,\mathrm{Hz}$ (*i.e.* $\lambda = 1\,\mu\mathrm{m}$).

If $F_{rad} = \frac{2}{3}\frac{e^2}{c^3}(d_{tt}\upsilon)$ is ignored, the energy loss in a bending unit will be proportional to $-eE * X_{exit} + eE * X_{entrance} = -eE * X_{exit}$ (because $X_{entrance}$ is taken as 0). Here, if the trajectory can be expressed as an equation $f(X, Y) = 0$, X_{exit} will satisfy $f(X_{exit}, W_y - L_y) = 0$. Actually, we can on purpose let $X_{exit} < 0$ by using a suitable value of $W_y - L_y$ and hence cause the energy loss to be a gain.

According to the formula on radiation power $\mathrm{Power} = \frac{2}{3}\frac{e^2}{mc^2}\frac{1}{mc}(d_t p)^2$, where $\frac{e^2}{mc^2} = 2.82 * 10^{15}\,\mathrm{m}$, we can find a relation between the ratio $\frac{\mathrm{Power}}{\mathrm{d}t\mathrm{Energy}}$ and the force felt by the particle: $\frac{\mathrm{Power}}{\mathrm{d}t\mathrm{Energy}} = \frac{\mathrm{Power}}{\mathrm{Force} * \upsilon} \sim \frac{2}{3}\frac{e^2}{mc^2}\frac{1}{mc}\frac{\mathrm{Force}}{c} * \frac{c}{\upsilon}$. Here, $\mathrm{d}t\mathrm{Energy} = \mathrm{Force} * \upsilon$ and $d_t p = \mathrm{Force}$. Clearly, Force is $\frac{120}{282} * 10^2 * \frac{c}{\upsilon}$ N if it is $\frac{\mathrm{Power}}{\mathrm{d}t\mathrm{Energy}} \sim 1$. For the strengths of E and B considered here, we have $\mathrm{Force} \sim 1.6 * 10^{-19+6}$ N and hence $\frac{\mathrm{Power}}{\mathrm{d}t\mathrm{Energy}} \sim 1.6 * 2.5 * 10^{-13-2} * \frac{\upsilon}{c}$, which means radiation loss *Power* is really negligible. Therefore, the energy loss due to F_{rad} is negligible for the case studied. It also means that the above-described hyperbolical and elliptical trajectories are robust relative to the effect due to F_{rad}.

We have described in details a more effective and simple way of controlling the size of a conventional solid-state accelerator. Completely relying on B_s to achieve a π-deflection is very space-consuming. In contrast, some reasonable methods of usage of E_s and B_s can achieve a π-deflection in a satisfactory small space. This suggests that it is possible for the most common conventional solid-state accelerator to have a table-top size. By using two $\frac{\pi}{2}$-deflections, we can make the electron run backward, and the forward path and the backward path are spaced by an adjustable distance (see fig. 3). The distance between two paths can be adjusted to a small value which is a practically meaningful level such as 0.1 m–0.01 m (a too small value is unnecessary because the size of whole apparatus (accelerating and bending regions) is also determined by the length of the accelerating region). Namely, the bending region can be of far smaller size than that of the accelerating region. Repeated usage of the accelerating region and the compactness of the bending region can warrant that the whole solid-state accelerator be at the table-size level.

* * *

This work is supported by National Science Fund No. 11374318, No. 11335013 and No. 11174305.

REFERENCES

[1] Chao Alexander W. *et al.*, *Handbook of Accelerator Physics and Engineering*, 2nd edition (World Scientific) 2013.
[2] Feder T., *Phys. Today*, **57**, issue No. 6 (2004) 30.
[3] Kolomenskii A. A., *JETP Lett.*, **6** (1967) 204.
[4] Sessler A. M., *Phys. Today*, **41**, issue No. 1 (1988) 26.
[5] Morozov A. I., Kislov A. Ya and Zubkov I. P., *JETP Lett.*, **7** (1968) 224.
[6] Tajima T. and Dawson J. M., *Phys. Rev. Lett.*, **43** (1979) 267.
[7] Scheid W. and Hora H., *Laser Part. Beams*, **7** (1989) 315.
[8] Kawata S., Maruyama T., Watanabe H. and Takahashi I., *Phys. Rev. Lett.*, **66** (1991) 2072.
[9] Hussein M. S., Pato M. P. and Kerman A. K., *Phys. Rev. A*, **46** (1992) 3562.
[10] Haaland C. M., *Opt. Commun.*, **114** (1995) 280.
[11] Sprangle P., Esarey E., Krall J. and Ting A., *Opt. Commun.*, **124** (1996) 69.
[12] Rau B., Tajima T. and Hojo H., *Phys. Rev. Lett.*, **78** (1997) 3310.
[13] Steinhauer L. C. and Kimura W. D., *J. Appl. Phys.*, **72** (1992) 3237.
[14] Hussein M. S. and Pato M. P., *Phys. Rev. Lett.*, **68** (1992) 1136.
[15] Bochove E. J., Moore G. T. and Scully M. O., *Phys. Rev. A*, **46** (1992) 6640; Scully M. O. and Zubairy M. S., *Phys. Rev. A*, **44** (1991) 2656.
[16] Hauser T., Scheid W. and Hora H., in *Laser Interaction and Related Plasma Phenomena*, edited by Miley G. H., *AIP Conf. Proc.*, **318** (1994) 20.
[17] Malka G., Lefebvre E. and Miquel J. L., *Phys. Rev. Lett.*, **78** (1997) 3314.
[18] Hartemann F. V., Fochs S. N., Le Sage G. P., Luhmann N. C., Woodworth J. G. jr., Perry M. D., Chen Y. J. and Kerman A. K., *Phys. Rev. E*, **51** (1995) 4833; Hartemann F. V., Van Meter J. R., Troha A. L., Landahl E. C., Luhmann N. C., Baldis H. A., Gupta A. and Kerman A. K., *Phys. Rev. E*, **58** (1998) 5001.
[19] Troha A. L., Van Meter J. R., Landahl E. C., Alvis R. M., Unterberg Z. A., Li K., Luhmann N. C., Kerman A. K. and Hartemann F. V., *Phys. Rev. E*, **60** (1999) 926.
[20] Ho Y. K., Wang J. X., Feng L., Scheid W. and Hora H., *Phys. Lett. A*, **220** (1996) 189.
[21] Goreslavsky S. P., Fedorov M. V. and Kilpio A. A., *Laser Phys.*, **5** (1995) 1020.
[22] Esarey E., Sprangle P. and Krall J., *Phys. Rev. E*, **52** (1995) 5443.
[23] Esarey E., Sprangle P., Krall J. and Ting A., *IEEE Trans. Plasma Sci.*, **24** (1996) 252 and references therein; Esarey E., Schroeder C. B. and Leemans W. P., *Rev. Mod. Phys.*, **81** (2009) 1229 and references therein.
[24] Flippo K., Hegelich B. M., Albright B. J. *et al.*, *Laser Part. Beams*, **25** (2007) 3.
[25] Yin L., Albright B. J., Heglich B. M. *et al.*, *Laser Part. Beams*, **24** (2006) 291.
[26] Bogomolov Ya. L., Litvak A. G. and Feigin A. M., *JETP Lett.*, **45** (1986) 12.
[27] Andreev N. E., Kirsanov V. I., Pogosova A. A., Gorbunov L. M., *JETP Lett.*, **60** (1994) 694.
[28] Joshi C. *et al.*, *Nature*, **311** (1984) 525.
[29] Takeuchi S., *Phys. Rev. E*, **66** (2002) 037402.
[30] Lawrence E. O., US patent 1948384, issued 1934-02-20.
[31] Friedman Y. and Semon M. D., *Phys. Rev. E*, **72** (2005) 026603.